Wohlmuth Da Silva, S.; Ortega Navarro, EM.; Siqueira Rodrigues, MA.; Moura Bernardes, A.; Pérez-Herranz, V. (01-0). Using p-Si/BDD anode for the electrochemical oxidation of norfloxacin. Journal of Electroanalytical Chemistry. 832:112-120. https://doi.org/10.1016/j.jelechem.2018.10.049

Using p-Si/BDD anode for the electrochemical oxidation of norfloxacin

Salatiel W. da Silvaa,[b], Emma M.O. Navarro[a], Marco A.S. Rodrigues[c], Andréa M. Bernardes[b,*], Valentín Pérez-Herranz[a]

[a] Grupo IEC, Departamento de Ingeniería Química y Nuclear, Universitat Politècnica de València, P.O. Box 22012, E-46071, Valencia, Spain

[b] Departamento de Materiais, PPGE3M, Universidade Federal do Rio Grande do Sul, Avenida Bento Gonçalves, 9500 Porto Alegre, Brazil

[c] Universidade Feevale, Campus II ERS-239, 2755 Novo Hamburgo, Brazil

* Corresponding author. e-mail address: amb@ufrgs.br (A.M. Bernardes).

Abstract.

This study evaluated the electrochemical advanced oxidation process (EAOP) using boron-doped diamond (p-Si/ BDD) anode in the abatement of the antibiotic norfloxacin (NOR). The influence of the applied current density (i_{app}), initial concentration of NOR, sodium sulfate (Na_2SO_4) concentration and reactor operation conditions were evaluated. The mechanism of NOR oxidation (direct or indirect) was also studied by cyclic voltammetry and chronoamperometry. The results showed that, depending on the i_{app}, and the NOR and Na_2SO_4 concentration, the NOR could be oxidized by direct electron transfer, with the carbon-sp^2 impurities on the p-Si/BDD surface, and indirect, by persulfate ions ($S_2O_8^{2-}$), sulfate ($SO_4^{\bullet-}$) and/or hydroxyl radicals ($HO^{\bullet}$) electrogenerated at the anode surface. When the reactor is operated favoring the electro-generated $HO^{\bullet}$, NOR abatement and chemical oxygen demand (COD) reduction are simultaneous. Conversely, at the time that the reactor is operated favoring the NOR direct oxidation and by $S_2O_8^{2-}$ and $SO_4^{\bullet-}$, NOR and COD reduction are not parallel leading to high byproducts formation. Therefore, it is important to know the matrix content (organic and sulfate content), for the correct choice of the operational parameters that will lead to a low byproducts formation.

Keywords: Electrochemical oxidation; p-Si/BDD electrode; Norfloxacin; Direct/indirect oxidation

1. Introduction.

The presence of contaminants of emerging concern (CEC), including pharmaceuticals and personal care products (PPCP), is increasingly being detected at low levels in water [1]. In the case of pharmaceuticals, the antibiotics are one of the main drugs used by humans and animals and reach the water bodies through ingestion and excretion of unmetabolized antibiotic, pharmaceutical and hospital wastewater, disposal of unused medicinal products either directly in the domestic sewage system and or by leaching from landfills [2].

The high discharge of antibiotics in water bodies is endangering the reuse of treated wastewater, usually a proposed solution to achieve sustainable management of the water cycle [3]. Studies have reported that fluoroquinolone antibiotics, such as norfloxacin (NOR), are the most frequently detected in Australia [4], Canada [5], Italy [6], Mexico [7], Sweden [8] and USA [9]. In studies conducted by Lindberg et al. [10] NOR was detected in 97% of samples in Sweden. Zorita et al. [8] reported a 70% effectiveness in removing NOR using coagulation/ flocculation operations. Furthermore, studies conducted by Kummerer [11] have shown that fluoroquinolones are not readily biodegradable.

Water recycling is reusing treated wastewater for beneficial purposes replenishing a ground water basin; water recycling can also offer resources and financial savings. However, wastewater treatment need to be tailored to meet the water quality requirements of a planned reuse [12]. For this propose, recycled water needs to be treated following standards, criteria and regulation. To this end, processes that are more efficient in removing CECs without the formation of toxic products need to be further studied.

In this context, Electrochemical Advanced Oxidation Process (EAOP) has been studied in the degradation of many organic compounds [13–15]. Nonetheless, the traditional anodes used in the EAOP process does not always lead to satisfactory current efficiencies or removal of organic contaminants without the formation of more toxic byproducts than the original ones. Boron-doped diamond (BDD) electrodes can fill these gaps when used as electrode material.

According to Kapałka et al. [16] BDD have technologically important features, including an inert surface with low adsorption properties, remarkable stability to corrosion even in strong acid, and extremely high overpotentials for oxygen evolution. Because of these properties, electrolysis in water discharge region of the BDD electrodes produces a high amount of hydroxyl radical ($HO^{\bullet}$) that is weakly adsorbed on the surface, and therefore has high reactivity for the oxidation of organic compounds (Eqs. (1), (2) and (3)) [17], enabling effective application for the treatment of water.

$$\mathrm{BDD} + \mathrm{H_2O} \rightarrow \mathrm{BDD}\,(\mathrm{HO^{\cdot}}) + \mathrm{H^+} + e^- \tag{1}$$

$$\mathrm{BDD_{(aq)}} + \mathrm{BDD}\,(\mathrm{HO^{\cdot}})_{\frac{n}{2}} \rightarrow \text{Oxidation products} + \frac{n}{2}\mathrm{H^+} + \frac{n}{2}e^- \tag{2}$$

$$\mathrm{BDD\,(HO^{\cdot})} \rightarrow \mathrm{BDD} + \frac{1}{2}\,\mathrm{O_2} + \mathrm{H^+} + e^- \qquad (3)$$

The NOR degradation by BDD anodes has already been reported in the literature [18]. Coledam et al. [18] evaluated the influence of initial pH (3, 7 and 10), temperature (10, 25 e 40 °C) and the diamond-sp^3/sp^2-carbon ratio aiming the degradation of 100 mg L^{-1} of NOR inbackground solution containing 0.1M of Na_2SO_4. It was found that the NOR oxidation was successfully attained with BDD anodes of distinct characteristics, independently of the solution pH, and at low current densities. The NOR oxidation was attributed to the hydroxyl radicals ($HO^{\bullet}$) and hydrogen peroxide (H_2O_2) electro-generated at BDD surface. Nevertheless, the indirect NOR oxidation by persulfate ions ($S_2O_8^{2-}$) and sulfate radicals ($SO_4^{\bullet-}$) electro-generated at the BDD surface [19–21] was not considered by the authors.

To fill this gap and elucidate how the direct or indirect electrolytic process affects NOR oxidation, cyclic voltammetry and chronoamperometry measurements were carried out with different NOR and Na_2SO_4 concentrations. After that, the abatement of the NOR by EAOP using a p-Si/BDD_{2500} anode was accomplished. The main operational factors such as applied current density (i_{app}), recirculation time, concentration of supporting electrolyte (Na_2SO_4, 0.01 and 0.5 M) and initial NOR concentration (10 and 30 mg L^{-1}) were evaluated. The kinetics, the mean values of the space-time yield and the accumulative current efficiency were also studied.

2. Material and methods

2.1. Chemicals

Norfloxacin was purchased in a local pharmacy (98%, Medley). Anhydrous sodium sulfate and sulfuric acid were of analytical grade supplied by Merck and Chemical Oxygen Demand (COD) reactants were from Panreac. Solutions were prepared with deionized water with a conductivity of 1 μS cm^{-1} at 25 °C.

2.2. Main characteristics of BDD electrode

Boron-doped diamond (BDD) electrodes were purchased from NeoCoat SA (Switzerland), where they were obtained by the hot filament chemical vapor deposition technique on p-Silicon substrate. A polycrystalline film with thickness of 3.1 μm and 2500 mg kg^{-1} boron concentration were obtained. The resistivity of the p-Si/BDD electrode was 14 mΩ cm, the uniformity within 100 mm (3σ) was ±5% and the diamond-sp^3/sp^2-carbon ratio was ~200. The values refer to the sp^3/sp^2 ratio determined by Raman spectroscopy, as provided by the manufacturer.

2.3. Voltammetry and chronoamperometry experiments

Electrochemical measurements were carried out using a conventional three-electrode cell with a capacity of 100 mL in conjunction with a computer-controlled potentiostat/galvanostat Auto lab model PGCTAT 302N. p-Si/BDD electrode with 0.19 cm^2 was used as the working electrode, Ag/AgCl (saturated) as a reference electrode and platinum (Pt) as the counter electrode. Voltammetric experiments were performed in unstirred solutions at scan rate of 100 mV s^{-1}, whereas chronoamperometric experiments were performed in stirred solutions (with magnetic bar) to prevent diffusion problems.

2.4. EAOP with p-Si/BDD electrode

The abatement of the antibiotic NOR was carried out in a single compartment electrochemical flow cell, described in Fig. 1. A p-Si/BDD electrode was used as the anode and stainless steel AISI 304 was used as the cathode. Both electrodes were square shaped with a geometric area of 100 cm^2 each and an electrode gap of 3 cm was used. The electrolyte was stored in a tank with capacity of 1 L and circulated through the electrolytic cell by means of a centrifugal pump with a flow rate of 30 L h^{-1}.

The assays were performed in galvanostatic mode at different applied current densities (i_{app}) of 5, 10 and 20 mA cm^{-2}, with two different solutions with NOR concentration of 0.031 (10 mg L^{-1}) or 0.1 Mm (30 mg L^{-1}), using a 0.01 or 0.5 M Na_2SO_4 as supporting electrolyte, at initial pH 4.0. No control of pH was carried out during the EAOP.

2.5. Analysis

According to Huang et al. [22] the NOR has a characteristic absorption spectrum and a maximum absorbance peak at 272 nm. Therefore, changes in the UV/Vis spectra of the NOR may indicate its degradation or the formation of reaction intermediates. In this sense, changes in the UV/Vis spectra were evaluated during the oxidation experiments by UV/Vis spectroscopy (UV4 ThermoSpectronic) using quartz cuvettes with 10 mm optical path. Besides the qualitative UV/Vis spectra changes, based on the 272 nm peak, a concentration curve versus absorbance was constructed and NOR abatement could be also monitored. Then, the fraction of NOR removal (XNOR, %) can be calculated by the Eq. (4):

$$X_{NOR} = \frac{C_0 - C}{C_0} \times 100 \quad (4)$$

where C_0 is the initial concentration of NOR and C is the concentration of NOR at any time, determined from the UV/Visible analysis at 272 nm.

Studies have shown that the degradation of various organic contaminants follows the pseudo-first order for recirculation systems with low contaminant concentrations (C_0 < 100 mg L^{-1}) [23–25]. Based on this information, the apparent kinetics (k_{app}, min^{-1}) for NOR abatement can be estimated by Eq. (5):

$$C = C_0 + e^{-k_{app} \times t} \quad (5)$$

where t is the time (min).

Chemical oxygen demand (COD, mg L^{-1} of O_2) was assessed by closed reflux colorimetric method according to the Standard Methods for the Examination of Water and Wastewater [26]. The fraction of COD reduction (XCOD, %) can be calculated by the equation:

$$X_{COD} = \frac{COD_0 - COD}{COD_0} \times 100 \quad (6)$$

where COD_0 is the initial concentration of COD and COD is the concentration of COD at any time.

The pH was measured by a microp H 2000 Crison.

For a better comprehension of the obtained results, the mean values of the space-time yield, (η, g L^{-1} h^{-1}), the accumulative current efficiency (ϕ), and the specific energy consumption (E_s, kW h kg^{-1}), referred to COD were also calculated according to the Eqs. (7)–(9) [27].

$$\eta = \frac{60 \times \Delta(COD)_{exp}}{t} \quad (7)$$

where COD_0 is the initial COD concentration (g of O_2 L^{-1}) and COD is the COD concentration at any time of treatment.

$$\phi = \frac{F \times V \times \Delta(COD)_{exp}}{8 \times \int_0^t I(t)dt} \quad (8)$$

where F is the Faraday constant (C mol^{-1}), V is the volume of solution (L) and I is the applied current (A).

$$E_s = \frac{\int_0^t E_{cell}(t) \times I(t)dt}{3600 \times V \times \Delta(COD)_{exp}} \quad (9)$$

where E is the cell voltage (V).

3. Results and discussion

3.1. Electrochemical measurements

Before starting the NOR electrolysis, cyclic voltammetric and chronoamperometric experiments were performed to achieve information regarding the NOR oxidation mechanism (direct or indirect). The cyclic voltammetric curves shown in Fig. 2 were obtained in aqueous solution adding step-by-step the supporting electrolyte (Na_2SO_4), without NOR, at a scan rate of 100 mV s^{-1}. As it can be seen in Fig. 2, a single irreversible anodic wave at ~2.1 V, before the oxygen evolution, is found and the peak current density (i_p) increases proportionally with the concentration of Na_2SO_4. This result shows the probable formation of persulfate ions ($S_2O_8^{2-}$) and sulfate radicals ($SO_4^{\bullet-}$), that should occur thought the reactions of electro-generated HO% (Eq. (10)) with sulfate anions (SO_4^{2-}), reactions (11) and (12). The $HO^{\bullet}$ has a short lifetime, and sp^2 sites present at the p-Si/BDD surface have high adsorption properties that can help the retention of SO_4^{2-} on the anode, improving the efficiency of $S_2O_8^{2-}$ and $SO_4^{\bullet-}$ generation [21,28].

$$H_2O \rightarrow HO^{\cdot} + H^+ + e^- \quad (10)$$

$$HSO_4^- + HO^{\cdot} \rightarrow SO_4^{\cdot-} + H_2O \quad (11)$$

$$2\,SO_4^{\cdot-} \rightarrow S_2O_8^{2-} + 2\,e^- \quad (12)$$

Therefore, is necessary to consider that the oxidation of NOR is not exclusively mediated by hydroxyl radicals but also by persulfate ions and sulfate radicals.

Fig. 3a shows the typical cyclic voltammetric curves obtained on a p-Si/BDD with the step-by-step injection of 0.31 M NOR in a 0.1 M Na_2SO_4 background solution. It is possible to observe at about 1.26 V an irreversible anodic shoulder corresponding to the oxidation of NOR. This means that NOR interact with the carbon-sp^2 in p-Si/BDD surface and a direct electron transfer will occur (direct oxidation) if the oxidation process is conducted at a potential in the water stability region (E < 2.106 V vs. Ag/AgCl).

To better visualize these results, Fig. 3b shows the expansion of Fig. 3a in the 1 to 1.5 V vs. Ag/AgCl region. The inset graph exhibited the relationship between the oxidation peak current density (i_p) and the concentration of NOR. At a scan rate of 100 mV s^{-1} the i_p is always proportional to the NOR concentration, meaning that the NOR oxidation in the p-Si/BDD is controlled by diffusion [29], which can be confirmed by the linear response observed in this range.

According to the cyclic voltammograms presented in Figs. 2 and 3, depending on the concentration ratio between Na_2SO_4 and NOR and the iapp, different situations marked in Fig. 3a can occur. For low i_{app}, if low overpotentials are reached (line 1), NOR oxidation take place by direct transfer of electrons with the carbon-sp2 in p-Si/BDD surface to form other organic products. For higher i_{app} (line 2), such that the reached overpotential coincides with Na_2SO_4 oxidation, indirect oxidation can occur by the $HO^{\bullet}$, $S_2O_8^{2-}$ and $SO_4^{\bullet-}$. Finally, if even larger iapp are used, in a way that very high overpotentials are

achieved (line 3), it is possible to favor the NOR abatement by the electro-generated $HO^{\bullet}$.

To achieve more information on the oxidation mechanism and to evaluate if any direct electron transfer reaction takes place on the surface of the p-Si/BDD electrode, chronoamperometric measurements by the step-by-step injection of NOR into the 0.1 M Na_2SO_4 solution at different potentials (1.260 and 2.406 V vs. Ag/AgCl) were carried out [30].

As shown in Fig. 4a (1.260 V vs. Ag/AgCl), an increase of the steady state current was observed, with an increasing concentration of NOR. Furthermore, the current density increases with a linear dependence on the NOR concentration (inset in Fig. 4a), suggesting the presence of direct electron-transfer. In fact, according to Zhi et al. [30], if the oxidation of organics occurs exclusively by the $HO^{\bullet}$, the current should be expected to depend with 1/[NOR]. Hence, in accordance with all these experimental facts, the present results clearly indicate that a direct electrochemical oxidation pathway can be at least partially attributed on the surface of the p-Si/BDD electrode.

Interestingly, when the chronoamperometric measurements were performed at 2.406 V vs. Ag/AgCl (Fig. 4b), a higher NOR concentration was necessary to observe a slight increase of the steady state current. As can be seen in Fig. 4b, at 2.406 V vs. Ag/AgCl, for the first NOR additions the steady state current decreased, but when more NOR is added the steady state current increase gradually. This fact shows the possible simultaneous occurrence of different processes: $HO^{\bullet}$ and $S_2O_8^{2-}$, $SO_4^{\bullet-}$ mediated reactions, a possible adsorption phenomenon (carbon-sp2 sites) and direct oxidation at the p-Si/BDD electrode surface, the last one being detectable in Fig. 3. According to Fig. 3a when high current densities are applied, $HO^{\bullet}$ and $S_2O_8^{2-}$, $SO_4^{\bullet-}$ mediated reactions are probably more favored with respect to direct oxidation.

3.2. EAOP of norfloxacin

Based on the results found in Fig. 3, the reactor was operated varying the ratio between NOR and supporting electrolyte (Na_2SO_4) at different applied current densities.

3.2.1. Effect of applied current density

The experiments aiming to evaluate the effect of the i_{app} (5, 10 and 20 mA cm^{-2}) were carried out in 0.01M of Na_2SO_4 background solution with 0.1mM NOR antibiotic. The first point observed during these experiments is that the cell potential was almost constant during each experiment, indicating that no significant deterioration or passivation phenomena occurs in the electrode.

Fig. 5a shows that for an i_{app} of 5 mA cm^{-2} there is a linear decrease of the NOR abatement while COD removal follows the same inclination up to 108 min, where a difference between the NOR abatement and COD removal can be visualized. When the

i_{app} was 10 mA cm^{-2}, the NOR abatement follows a parallel and linear tendency to COD removal from the beginning of the EAOP until the final time of 144 min.

On the other hand, when the i_{app} is 20 mA cm^{-2} one can observe that the NOR abatement runs parallel to the COD removal until the end of the EAOP and, after 36 min of oxidation, NOR abatement and COD removal begins to be exponential. This means that by applying a current of 5 or 10 mA cm^{-2} the process is not kinetically limited by mass transport, meanwhile, when 20 mA cm^{-2} are applied there is a mixed kinetic regime.

This behavior can be explained because at low i_{app}, this system would be working in the points 1 and/or 2 marked in Fig. 3a, meaning that the oxidation of NOR occurs by direct electrons transfer with the carbon-sp^2 atoms on BDD surface and by mediated reactions by the persulfate ions and sulfate radicals. For higher i_{app}, the system would be working at the point 3 marked in Fig. 3a, where NOR oxidation occurs primarily by hydroxyl radicals formed in these conditions. In this case the NOR abatement and COD removal is parallel, while in the above cases, the NOR abatement is faster than COD removal.

The smaller NOR abatement and COD removal when a lower current is applied can be explained because after a certain treatment time NOR is not the only organic component in the solution. In fact, the remaining byproducts may be more resistant to oxidation than the parent one. Besides, due to the low concentration of organic, diffusion problems can occur. On the other hand, the increase on the applied current led to an increase in NOR abatement and COD removal. This increase in NOR abatement and COD removal can be related to the formation of strong oxidizing species ($HO^{\bullet}$ generated, point 3 marked in Fig. 3a), and to the oxygen evolution reactions, that can promote the hydrodynamic conditions, thus minimizing the mass transport limitations.

The inset graph suggests the same, i.e. increasing the i_{app} there is also an increase in the rate constant values calculated at the final time using the Eq. (5). In the operational parameters of EAOP experiments, for all i_{app}, analysis of the above NOR concentration abatement by means of kinetic Eq. (5) related to simple reaction orders revealed that they followed a pseudo-first-order. From the representation of ln (C/C_0) as a function of the time shown in Fig. 4b, a rate constant (k') of 0.0044, 0.0060 and 0.0208 min^{-1} was calculated for 5, 10 and 20 mA cm^{-2}, respectively. The pseudo-first-order abatement for NOR is typical of the removal of aromatics by EAOP [31] and can be explained by the quasi-steady content achieved for HO% since these species cannot be accumulated in the anode surface or in the bulk solution because they have a very short lifetime [32].

3.2.2. Effect of initial norfloxacin concentration and applied current densities

The experiments aiming to evaluate the effect of the initial NOR concentration and i_{aap} were carried out in 0.01 M of Na_2SO_4 background solution with 0.031 and 0.1 mM of NOR, and different i_{app} of 5, 10 and 20 mA cm^{-2}.

In Fig. 6, two different behaviors can be observed as a function of the NOR concentration. For a lower NOR concentration (0.031 mM) there is a higher NOR abatement (Fig. 6a), whereas for a higher concentration of NOR (0.1 mM), a higher COD

removal is observed (Fig. 6b). In fact, the small difference in the results comparing the NOR concentrations do not seem to have a higher influence on the results of the EAOP. However, this behavior can be explained in terms of the mechanisms that control the electrochemical processes [33].

In the EAOP of concentrated contaminants, the process can be considered kinetically controlled for a significant time [34,35]. The electro-generation of oxidants in the anode surface is not enough to oxidize all NOR molecules that reach this zone. Under these conditions, direct oxidation and $HO^{\bullet}$ indirect oxidation are favored over the oxidation by other electro-generated oxidants and consequently a higher COD removal is achieved. On the other hand, mass transfer controls the EAOP of more diluted contaminants. The concentration of oxidizing agents formed in the anode surface is very high compared to the amount of NOR that reaches the anode surface, and the short lifetime of $HO^{\bullet}$ favors the formation of hydrogen peroxide or the oxygen evolution reaction with a subsequent reduction in current efficiency. Consequently, the persulfate ions and sulfate radicals are formed from the salts present in the electrolyte and this oxidant may act in the anode surface and in the bulk solution, enhancing the NOR abatement, although the overall process efficiency tends to decrease [36].

Fig. 7a shows that in all cases the space-time yield (η, g L^{-1} h^{-1}) increases with the i_{app}. However, the evolution with time depends on the applied current densities and the NOR concentration. For more diluted NOR concentration (0.031 mM), the evolution of space-time yield calculated from COD results (Fig. 7a) shows an exponential decrease with time for the i_{app} of 10 and 20 mA cm^{-2}. According to García-Gabaldón et al. [27], these results can be explained because when the i_{app} is higher than the limiting one, an exponential decrease is expected, since under this situation the contaminants are removed from the solution at the maximum reaction rate.

In addition, the exponential shape of Fig. 7a usually is explained in terms of mass-transfer limitations (in the range of NOR concentration studied in this work), assuming that both direct oxidation on the p-Si/BDD surface and mediated oxidation by $HO^{\bullet}$ and other oxidants electro-generated from the supporting electrolyte contribute to the electrochemical process [37–39]. On the other hand, for the i_{app} of 5 mA cm^{-2}, a linear shape can be noted. This means that, in this case, the EAOP was conducted at currents lower than the limiting one and the contaminants are under current control. Additionally, with the reactor operating with an applied current above the limiting one, there is an increase of the space-time yield related to the increase on the applied current. This can be explained by a higher generation of O_2 at the anode and H_2 on the cathode, promoting higher turbulence.

In contrast, for higher NOR concentration (0.1 mM) the specific yield remains practically constant over the time for all i_{app}, which would be an indication that in this case the reactor would be working below the limiting current, corresponding to the generation of $HO^{\bullet}$, and that the process is not under control by mass transfer.

The results of accumulative current efficiency calculated from COD results (ϕ) (Fig. 7b) shows that an increase in the i_{app} does not lead to an increase in the current efficiency

of the oxidation process. Generally, in the low applied current range, when the EAOP is not kinetically limited by the mass transport of the contaminants to the anode surface, an increase in i_{app} leads to higher contaminant removal. On the other hand, in the high applied current range, when the process is mass transport controlled, an increase in applied current enhance the reaction of O_2 evolution, thus giving rise to a decrease in current efficiency. For intermediate i_{app} values, when the process is under a mixed kinetic regime, higher i_{app} values should cause an increase in the contaminant removal but also a decay in current efficiency [35].

The low current efficiency values obtained are typical of processes in which the organic contaminant concentration is very low [35,36]. Furthermore, the low current efficiency values observed are related to secondary reactions, such as the generation of oxygen through the $HO^{\bullet}$ formed on the anode surface, which were not used in the NOR oxidation (Eq. (13)), the sulfate oxidation (Eqs. (11)–(12)), the electro-generation of hydrogen peroxide (Eq. (14)) and the hydrogen peroxide oxidation by hydroxyl radicals (Eq. (15)) [31,37].

$$2\,\mathrm{BDD}(\mathrm{HO}^{\bullet}) \rightarrow 2\,\mathrm{BDD} + \mathrm{O}_{2\,(g)} + \mathrm{H}^{+} + e^{-} \quad (13)$$

$$2\,\mathrm{BDD}(\mathrm{HO}^{\bullet}) \rightarrow 2\,\mathrm{BDD} + \mathrm{H_2O_2} \quad (14)$$

$$\mathrm{H_2O_2} + 2\,\mathrm{BDD}(\mathrm{HO}^{\bullet}) \rightarrow \mathrm{BDD}(\mathrm{H_2O}) + \mathrm{H_2O} \quad (15)$$

Moreover, in smaller concentrations of NOR (0.031 mM) there is also a reduction in the current efficiency. The COD removal in diluted NOR solutions decreases exponentially with time to 10 and 20 mA cm^{-2} and this behavior is characteristic of mass-transfer controlled processes. The smaller concentration cannot enhance the rate of oxidation of the organics at the electrode but rather favors anodic side reactions [30,38]. The low values of ϕ can also be attributed to the low presence of the NOR in solution and/or to the generation of more persistent byproducts, that is, products that will react more slowly with hydroxyl radicals and sulfate radicals, electro-generated in the anode surface.

Fig. 7c shows that for lower NOR concentrations (0.031 mM) the specific energy consumption is higher when compared to the values calculated for higher NOR concentrations (0.1 mM). This phenomenon can be attributed to hydrogen and oxygen evolution, causing, consequently, an energy consume increase.

3.2.3. Influence of supporting electrolyte concentration and applied current densities

The influence of supporting electrolyte concentration (Na_2SO_4, 0.01 and 0.5 M) was evaluated using a NOR concentration of 0.1mM and i_{app} of 10 or 50 mA cm^{-2}. Fig. 8 shows that the NOR abatement increased with the increase of Na_2SO_4 concentration, but the similar tendency of COD removal was not observed. When the concentration of Na_2SO_4 increased from 0.01 to 0.5 M, the ionic force and conductivity of the solution favors the movement of generated ions and the transport of strong oxidants from the surface of

the anode to the bulk of the solution, leading to an increased removal efficiency [39]. Meanwhile, when the concentration of Na_2SO_4 is higher, more anions would move to the anode under the influence of electric field. Therefore, the number of active sites of the electrode would be reduced, causing a decrease tendency of abatement efficiency [40].

Studies carried out by Lin et al. [41] demonstrated that the higher electrolyte concentration, the lower cell voltage, which can reduce the power consumption. On the other hand, according to the energy-band theory, the low voltage may not provide sufficient potential to activate electron transfer and thus reduces the COD removal. It is also important to note that an increase in current density from 10 to 50 mA cm^{-2} does not enhance the oxidation efficiency or oxidation rate (COD removal) since it favored the occurrence of the oxygen evolution reaction and/or of mass transport limitations.

In the meantime, it is demonstrated in the cyclic voltammetry studies that other strong oxidizing species can also be electro-generated in the p-Si/BDD surface, such as the $SO_4^{\bullet-}$ and $S_2O_8^{2-}$ coming from the oxidation of the anion of the supporting electrolyte. Consequently, the high-applied current density can favor mediated oxidation less by $HO^{\bullet}$ electro-generated from water decomposition and more by $SO_4^{\bullet-}$ and $S_2O_8^{2-}$ electro-generated from supporting electrolyte. Then $SO_4^{\bullet-}$ and $S_2O_8^{2-}$ can act in the electrode surface and in the bulk of solution increasing the NOR abatement and the reaction rate showing a pseudo-first order kinetics (inset graph), which not leads to the complete oxidation to CO_2 but rather to more resistant byproduct formation. The k_{app} value estimated from Eq. (5) for distinct Na_2SO_4 concentrations (0.01 and 0.5 M) and, at the same i_{aap} were 0.0060 and 0.0369 min^{-1}, respectively. For 0.5M of Na_2SO_4 and 50 mA cm^{-2} it was not possible to estimate the k_{app} value, because at 36 min there is no NOR present in the solution.

Fig. 9 shows the changes in UV/Vis spectra for the different samples obtained during the EAOP. This analytical technique can give qualitative information about the formation of byproducts and thus information on the oxidation routes. As it can be seen in Fig. 9a, when the EAOP conditions were 0.01 M of Na_2SO_4 and the i_{app} is 10 mA cm^{-2}, UV/Vis spectrum showed a small peak in 192 nm (1) and 210 nm (2), one peak in 272 nm (3) and a shoulder that begins at approximately 305 nm and ends at 330 nm (4). It is noted that with the time passing the intensity of all peaks decreases proportionally.

On the other hand, by increasing the amount of Na_2SO_4 from 0.01 to 0.5 M (Fig. 9b) there is an increase of the peak 1 and peak 2 and a decrease of the peaks 3 and 4. Consequently, the increased in the peak 1 can be attributed to protonated form, or vice versa (pH increased, Fig. 10) and peak 2 can be linked to the formation of byproducts. Moreover, when the i_{app} is 50 mA cm^{-2} (Fig. 9c) there is a complete removal of peaks 3 and 4 in the first 36 min. However, it is explicit the byproducts formation which can be viewed in a peak 2 at approximately 210 nm (that can be associated to carboxylic acids from decarboxylation of NOR [42]) and the protonated/unprotonated effect in the peak 1. These results indicate that the oxidation of NOR can lead to the formation of byproducts prior to the formation of carbon dioxide, what justifies the changes in the COD removal and NOR abatement values previously discussed.

These results can also be linked to the marked points in Fig. 3a. For the lowest concentration of the Na_2SO_4 (0.01 M) and the iapp of 10 mA cm^{-2}, the reactor was being operated in the point 3 of voltammogram, where the formation of $HO^{\bullet}$ is facilitated and NOR oxidation occurs primarily by these radicals, in which case the COD decreases more than in other cases.

When the concentration of the electrolyte increased to 0.5 M, the reactor would be operated in the point 2 of voltammogram, in a way that NOR is oxidized by direct electron transfer on carbon-sp^2 content on the p-Si/BDD surface, $SO_4^{\bullet-}$ and $S_2O_8^{2-}$, generating byproducts previously mentioned (modification in the UV/Vis spectra, Fig. 9a, b and c). In the latter case, the process was controlled by mass transfer of NOR, therefore C/C_0 decreases exponentially and COD removal is less than the NOR abatement.

In addition, for the concentration of 0.5 M of Na_2SO_4, when the i_{app} is increased from 10 to 50 mA cm^{-2}, the NOR abatement reaction rate increases. However, the COD removal is even smaller. This is in accordance with previously mentioned, i.e. the reactor is being operated at the point 2 marked on the voltammogram and the NOR oxidation occurs fundamentally by $SO_4^{\bullet-}$ and $S_2O_8^{2-}$, leading to incomplete oxidation of NOR what agrees to the results showing that peak 2 marked in the UV spectra, is higher for the highest applied current.

From the Figs. 8 and 9a, b and c, it is possible to conclude that the fast NOR abatement associated to the low COD removal, when 0.5 M of Na_2SO_4 was used, lead to intermediate products formation, causing an increase in the pH values that can be observed in Fig. 10. As presented in the literature [43], a possible mechanism for generating sulfate radicals is through the interaction of the sulfate present in the solution with the hydroxyl radical (Eq. (16)), resulting in sulfate radicals and hydroxyl. By increasing the amount of sulfate (Eq. (16)) and the applied current (what will result in a water splitting process as described by reaction 17) [43], there may be an increase of hydroxyls concentration in solution, shifting the pH to higher values.

$$SO_4^{2-} + HO^{\cdot} \rightarrow SO_4^{\cdot-} + OH^- \quad (16)$$

$$2\,H_2O + 4\,e^- \rightarrow H_2 + 2\,OH^- \quad (17)$$

4. Conclusions

The ratio between Na_2SO_4 and the NOR concentration as well as the i_{app} leads to different situations. For low i_{app}, if low overpotentials are reached, NOR oxidation take place by direct transfer of electrons with carbon-sp2 atoms on the p-Si/BDD surface to form byproducts. For higher i_{app}, such that the reached overpotential coincides with Na_2SO_4 oxidation, mediated oxidation can occur from the $SO_4^{\bullet -}$ and $S_2O_8^{2-}$ formed leading to a higher byproducts formation. Finally, if even larger current densities are applied, in a way that very high overpotentials are achieved, it is possible to generate $HO^{\bullet}$, and simultaneous NOR abatement and COD removal was achieved. Therefore, the choice of the correct parameters can improve the process efficiency and prevent the formation of unwanted byproducts.

Acknowledgements

The authors thank Cyted, CNPq, CAPES/DGPU project no. 7595/14-0, FAPERGS and FINEP. The authors thank the financial support from MINECO (Ministerio de Economía y Competitividad, Spain) under project CTQ2015-65202-C2-1-R, co-financed with FEDER funds.

References

[1] EPA, Contaminants of emerging concern including pharmaceuticals and personal care products, 1–2 https://www.epa.gov/wqc/contaminants-emerging-concernincluding- pharmaceuticals-and-personal-care-products, (2015), Accessed date: 30 March 2016.

[2] C.G. Daughton, T.A. Ternes, Pharmaceuticals and personal care products in the environment: agents of subtle change? Environ. Health Perspect. 107 (1999) 907, https://doi.org/10.2307/3434573.

[3] I. Muñoz, A. Rodríguez, R. Rosal, A.R. Fernández-Alba, I. Munoz, A. Rodriguez, R. Rosal, A.R. Fernandez-Alba, Life Cycle Assessment of urban wastewater reuse with ozonation as tertiary treatment. A focus on toxicity-related impacts, Sci. Total Environ. 407 (2009) 1245–1256, https://doi.org/10.1016/j.scitotenv.2008.09.029.

[4] S.D. Costanzo, J. Murby, J. Bates, Ecosystem response to antibiotics entering the aquatic environment, Special issue: Catchment to Reef: Water Quality Issues in the Great Barrier Reef Region, Mar. Pollut. Bull. 51 (2005) 218–223 34 ref https://doi.org/10.1016/j.marpolbul.2004.10.038.

[5] X.S. Miao, F. Bishay, M. Chen, C.D. Metcalfe, Occurrence of antimicrobials in the final effluents of wastewater treatment plants in Canada, Environ. Sci. Technol. 38 (2004) 3533–3541, https://doi.org/10.1021/es030653q.

[6] E. Zuccato, S. Castiglioni, R. Fanelli, Identification of the pharmaceuticals for human use contaminating the Italian aquatic environment, J. Hazard. Mater. 122 (2005) 205–209, https://doi.org/10.1016/j.jhazmat.2005.03.001.

[7] K.D. Brown, J. Kulis, B. Thomson, T.H. Chapman, D.B. Mawhinney, Occurrence of antibiotics in hospital, residential, and dairy effluent, municipal wastewater, and the Rio Grande in New Mexico, Sci. Total Environ. 366 (2006) 772–783, https://doi.org/10.1016/j.scitotenv.2005.10.007.

[8] S. Zorita, L. Mårtensson, L. Mathiasson, Occurrence and removal of pharmaceuticals in a municipal sewage treatment system in the south of Sweden, Sci. Total Environ. 407 (2009) 2760–2770, https://doi.org/10.1016/j.scitotenv.2008.12.030.

[9] K.G. Karthikeyan, M.T. Meyer, Occurrence of antibiotics in wastewater treatment facilities in Wisconsin, USA, Sci. Total Environ. 361 (2006) 196–207, https://doi.org/10.1016/j.scitotenv.2005.06.030.

[10] R.H. Lindberg, U. Olofsson, P. Rendahl, M.I. Johansson, M. Tysklind, B.A.V. Andersson, Behavior of fluoroquinolones and trimethoprim during mechanical, chemical, and active sludge treatment of sewage water and digestion of sludge, Environ. Sci. Technol. 40 (2006) 1042–1048, https://doi.org/10.1021/es0516211.

[11] K. Kummerer, Significance of antibiotics in the environment, J. Antimicrob. Chemother. 52 (2003) 5–7, https://doi.org/10.1093/jac/dkg293.

[12] USEPA, Guidelines for Water Reuse. EPA/625/R-04/108, Epa/625/R-04/108, (2004), pp. 1–28.

[13] J.M. Aquino, R.C. Rocha-Filho, C. Sáez, P. Cañizares, M.A. Rodrigo, High efficiencies in the electrochemical oxidation of an anthraquinonic dye with conductive diamond anodes, Environ. Sci. Pollut. Res. 21 (2014) 8442–8450, https://doi.org/10.1007/s11356-014-2784-0.

[14] O. Scialdone, A. Galia, S. Sabatino, Abatement of Acid Orange 7 in macro and micro reactors. Effect of the electrocatalytic route, Appl. Catal. B Environ. 148–149 (2014) 473–483, https://doi.org/10.1016/j.apcatb.2013.11.005.
[15] F. Sopaj, M.A. Rodrigo, N. Oturan, F.I. Podvorica, J. Pinson, M.A. Oturan, Influence of the anode materials on the electrochemical oxidation efficiency. Application to oxidative degradation of the pharmaceutical amoxicillin, Chem. Eng. J. 262 (2015) 286–294, https://doi.org/10.1016/j.cej.2014.09.100.
[16] A. Kapałka, G. Fóti, C. Comninellis, The importance of electrode material in environmental electrochemistry. Formation and reactivity of free hydroxyl radicals on boron-doped diamond electrodes, Electrochim. Acta 54 (2009) 2018–2023, https://doi.org/10.1016/j.electacta.2008.06.045.
[17] A. Kapałka, G. Fóti, C. Comninellis, Basic principles of the electrochemical mineralization of organic pollutants for wastewater treatment, in: C. Comninellis, G. Chen (Eds.), Electrochem. Environ. Springer New York, 2010, pp. 1–23, https://doi.org/10.1007/978-0-387-68318-8_1.
[18] D.A.C. Coledam, J.M. Aquino, B.F. Silva, A.J. Silva, R.C. Rocha-Filho, Electrochemical mineralization of norfloxacin using distinct boron-doped diamond anodes in a filter-press reactor, with investigations of toxicity and oxidation byproducts, Electrochim. Acta 213 (2016) 856–864, https://doi.org/10.1016/j.electacta.2016.08.003.
[19] S. Garcia-Segura, E. Vieira dos Santos, C.A. Martínez-Huitle, Role of sp^3/sp^2 ratio on the electrocatalytic properties of boron-doped diamond electrodes: a mini review, Electrochem. Commun. 59 (2015) 52–55, https://doi.org/10.1016/j.elecom.2015.07.002.
[20] J.P. de P. Barreto, K.C.d.F. Araujo, D.M. de Araujo, C.A. Martinez-Huitle, Effect of sp3/sp2 ratio on boron doped diamond films for producing persulfate, ECS Electrochem. Lett. 4 (2015) E9–E11, https://doi.org/10.1149/2.0061512eel.
[21] J. Davis, J.C. Baygents, J. Farrell, Understanding persulfate production at boron doped diamond film anodes, Electrochim. Acta 150 (2014) 68–74, https://doi.org/10.1016/j.electacta.2014.10.104.
[22] K.J. Huang, C.X. Xu, W.Z. Xie, Electrochemical behavior of norfloxacin and its determination at poly(methyl red) film coated glassy carbon electrode, Bull. Kor. Chem. Soc. 29 (2008) 988–992, https://doi.org/10.5012/bkcs.2008.29.5.988.
[23] L. Wang, J. Fu, Q. Qiao, Y. Zhao, Kinetic modeling of electrochemical degradation of phenol in a three-dimension electrode process, J. Hazard. Mater. 144 (2007) 118–125, https://doi.org/10.1016/j.jhazmat.2006.09.091.
[24] M.T. Fukunaga, J.R. Guimarães, R. Bertazzoli, Kinetics of the oxidation of formaldehyde in a flow electrochemical reactor with TiO2/RuO2 anode, Chem. Eng. J. 136 (2008) 236–241, https://doi.org/10.1016/j.cej.2007.04.006.
[25] M.H. Priya, G. Madras, Kinetics of photocatalytic degradation of phenols with multiple substituent groups, J. Photochem. Photobiol. A Chem. 179 (2006) 256–262, https://doi.org/10.1016/j.jphotochem.2005.08.022.
[26] E.W. Rice, R.B. Baird, A.D. Eaton, L.S. Clesceri, 5220 chemical oxygen demand (Cod), in: L.S.C.E.W. Rice, R.B. Baird, A.D. Eaton (Eds.), Stand. Methods Exam. Water Wastewater, American Public Health Association, American Water Works Association, Water Environment Federation, 2012, pp. 1–6 https://www.standardmethods.org/store/ProductView.cfm?ProductID=37.

[27] M. García-Galbadón, V. Pérez-Herranz, J. García-Antón, J.L. Guiñón, Electrochemical recovery of tin from the activating solutions of the electroless plating of polymers: galvanostatic operation, Sep. Purif. Technol. 51 (2006) 143–149, https://doi.org/10.1016/j.seppur.2005.12.028.

[28] C.D.N. Brito, D.M. De Araújo, C.A. Martínez-Huitle, M.A. Rodrigo, Understanding active chlorine species production using boron doped diamond films with lower and higher sp^3/sp^2 ratio, Electrochem. Commun. 55 (2015) 34–38, https://doi.org/10.1016/j.elecom.2015.03.013.

[29] B. Boye, E. Brillas, B. Marselli, P.-A. Michaud, C. Comninellis, G. Farnia, G. Sandonà, Electrochemical incineration of chloromethylphenoxy herbicides in acid medium by anodic oxidation with boron-doped diamond electrode, Electrochim. Acta 51 (2006) 2872–2880, https://doi.org/10.1016/j.electacta.2005.08.019.

[30] J.-F. Zhi, H.-B. Wang, T. Nakashima, T.N. Rao, A. Fujishima, Electrochemical incineration of organic pollutants on boron-doped diamond electrode. Evidence for direct electrochemical oxidation pathway, J. Phys. Chem. B 107 (2003) 13389–13395, https://doi.org/10.1021/jp030279g.

[31] I. Sirés, E. Brillas, M.A. Oturan, M.A. Rodrigo, M. Panizza, Electrochemical advanced oxidation processes: today and tomorrow. A review, Environ. Sci. Pollut. Res. 21 (2014) 8336–8367, https://doi.org/10.1007/s11356-014-2783-1.

[32] A. Dirany, I. Sirés, N. Oturan, A. Özcan, M.A. Oturan, Electrochemical treatment of the antibiotic sulfachloropyridazine: kinetics, reaction pathways, and toxicity evolution, Environ. Sci. Technol. 46 (2012) 4074–4082, https://doi.org/10.1021/es204621q.

[33] P. Cañizares, J. Lobato, R. Paz, M.A. Rodrigo, C. Sáez, Electrochemical oxidation of phenolic wastes with boron-doped diamond anodes, Water Res. 39 (2005) 2687–2703, https://doi.org/10.1016/j.watres.2005.04.042.

[34] M. Panizza, P.A. Michaud, G. Cerisola, C. Comninellis, Anodic oxidation of 2-naphthol at boron-doped diamond electrodes, J. Electroanal. Chem. 507 (2001) 206–214, https://doi.org/10.1016/S0022-0728(01)00398-9.

[35] C.A. Martínez-Huitle, M.A. Rodrigo, I. Sirés, O. Scialdone, Single and coupled electrochemical processes and reactors for the abatement of organic water pollutants: a critical review, Chem. Rev. 115 (2015) 13362–13407, https://doi.org/10.1021/acs.chemrev.5b00361.

[36] F.C. Moreira, R.A.R. Boaventura, E. Brillas, V.J.P. Vilar, Electrochemical advanced oxidation processes: a review on their application to synthetic and real wastewaters, Appl. Catal. B Environ. 202 (2017) 217–261, https://doi.org/10.1016/j.apcatb.2016.08.037.

[37] I. Sirés, E. Brillas, Remediation of water pollution caused by pharmaceutical residues based on electrochemical separation and degradation technologies: a review, Environ. Int. 40 (2012) 212–229, https://doi.org/10.1016/j.envint.2011.07.012.

[38] M. Panizza, P.A. Michaud, G. Cerisola, C.H. Comninellis, Electrochemical treatment of wastewaters containing organic pollutants on boron-doped diamond electrodes: prediction of specific energy consumption and required electrode area, Electrochem. Commun. 3 (2001) 336–339, https://doi.org/10.1016/S1388-2481(01)00166-7.

[39] C. Zhong, K. Wei, W. Han, L. Wang, X. Sun, J. Li, Electrochemical degradation of tricyclazole in aqueous solution using Ti/SnO2-Sb/PbO2 anode, J. Electroanal. Chem. 705 (2013) 68–74, https://doi.org/10.1016/j.jelechem.2013.07.027.
[40] J. Chen, Y. Xia, Q. Dai, Electrochemical degradation of chloramphenicol with a novel Al doped PbO2 electrode: performance, kinetics and degradation mechanism, Electrochim. Acta 165 (2015) 277–287, https://doi.org/10.1016/j.electacta.2015.02.029.
[41] H. Lin, J. Niu, S. Ding, L. Zhang, Electrochemical degradation of perfluorooctanoic acid (PFOA) by Ti/SnO2-Sb, Ti/SnO2-Sb/PbO2 and Ti/SnO2-Sb/MnO2 anodes, Water Res. 46 (2012) 2281–2289, https://doi.org/10.1016/j.watres.2012.01.053.
[42] H. Guo, T. Ke, N. Gao, Y. Liu, X. Cheng, Enhanced degradation of aqueous norfloxacin and enrofloxacin by UV-activated persulfate: kinetics, pathways and deactivation, Chem. Eng. J. 316 (2017) 471–480, https://doi.org/10.1016/j.cej.2017.01.123.
[43] S. Vasilie, F. Manea, A. Baciu, A. Pop, Dual use of boron-doped diamond electrode in antibiotics-containing water treatment and process control, Process. Saf. Environ. Prot. 117 (2018) 446–453, https://doi.org/10.1016/j.psep.2018.05.024.

FIGURES

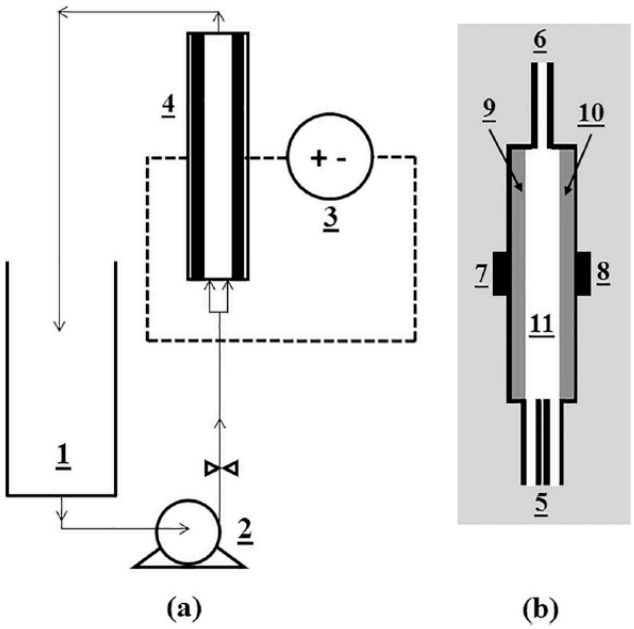

Fig. 1. Scheme of the reactor used for bulk oxidation of NOR on BDD anode. (a) Set up used: 1 is a reservoir, 2 is a pump, 3 is a power supply and 4 is the electrochemical cell. (b) Electrochemical cell: 5 is the electrolyte inlet, 6 is the electrolyte outlet, 7 and 8 are the electrical connections, 9 is the BDD anode, 10 is AISI 304 L cathode and 11 is the electrolysis compartment.

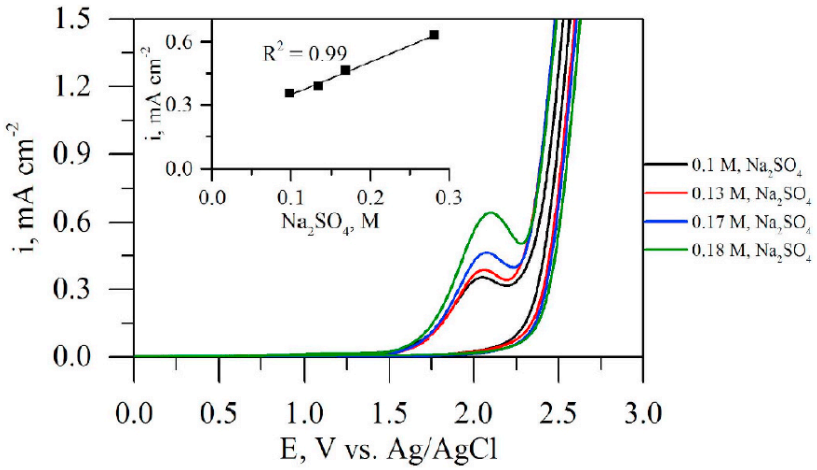

Fig. 2. Cyclic voltammogram response of p-Si/BDD by adding Na_2SO_4 step-bystep at scan rate of 100 mV s^{-1}. Inset graph shows the relationship between peak current density (i_p) and the Na_2SO_4 concentration.

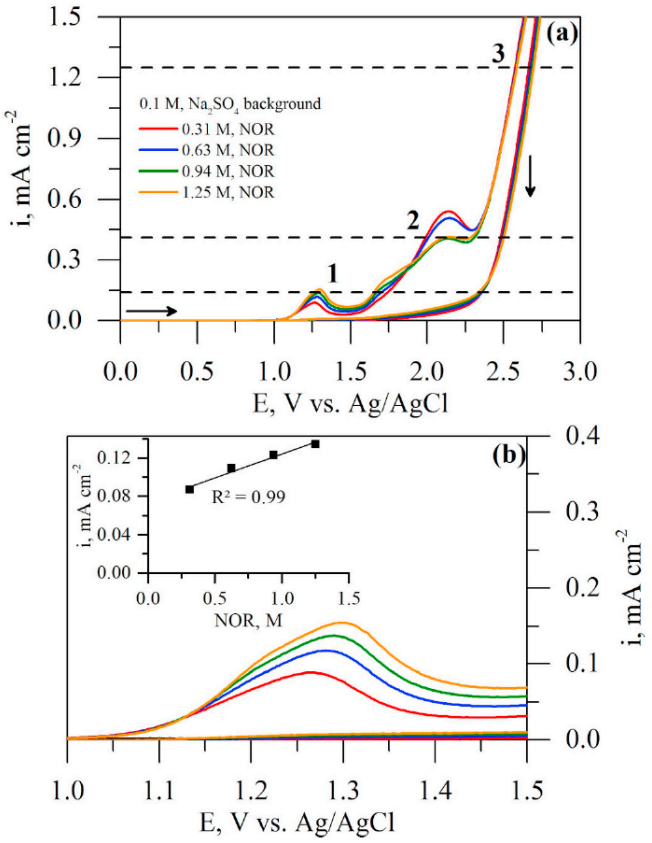

Fig. 3. Cyclic voltammogram response of p-Si/BDD (a) step-by-step injection of 0.31 M of NOR in 0.1 M of Na_2SO_4 background solution at scan rate of 100 mV s^{-1}, and (b) the amplification of irreversible anodic wave corresponding to direct electron transfer between NOR and p-Si/BDD surface. Inset graph shows the relationship between peak current density and the NOR concentration.

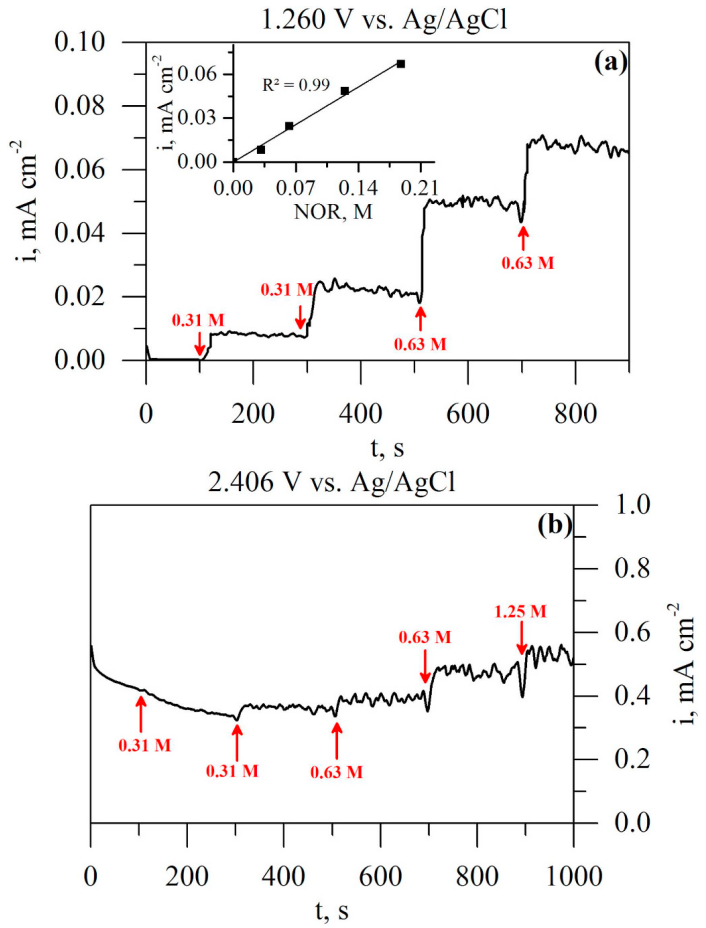

Fig. 4. Chronoamperometric response of p-Si/BDD electrode to step-by-step injection of NOR in a 0.1 M of Na_2SO_4 background solution at different potentials: (a) 1.260 V vs. Ag/AgCl and (b) 2.406 V vs. Ag/AgCl. Inset shows the correspondent ip as a function of NOR concentration.

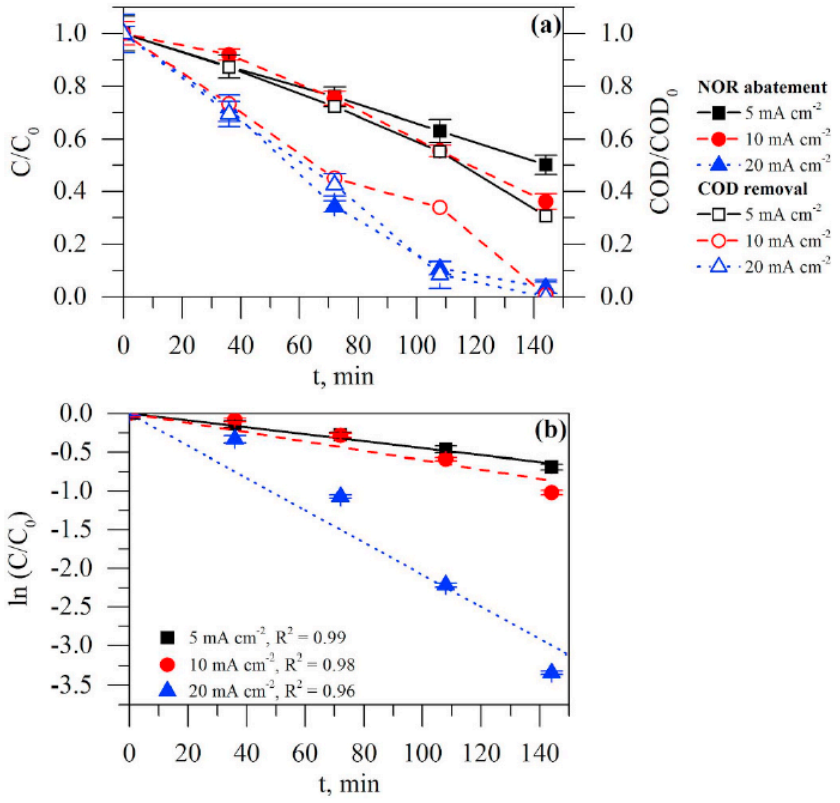

Fig. 5. Influence of the i_{app} in the (a) NOR abatement and COD removal. (b) Natural logarithm of C/C_0 as function of the time. EAOP initial conditions: 0.1 mM of NOR in 0.01 M of Na_2SO_4 background solution, pH 4 at 25 °C.

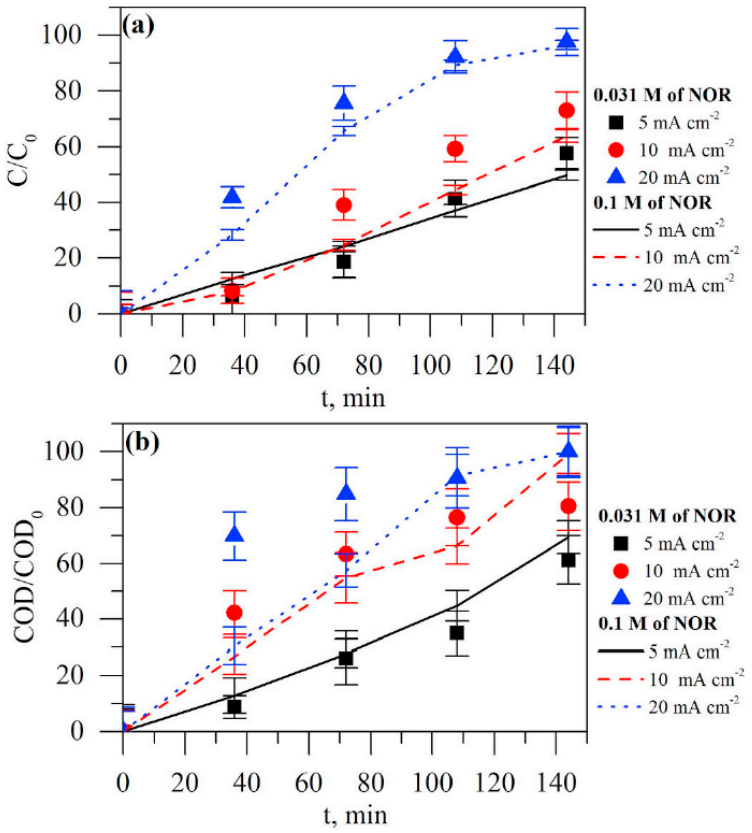

Fig. 6. Influence of the NOR concentration and i_{app} in the (a) NOR abatement and (b) COD removal. EAOP initial conditions: 0.031 or 0.1 mM of NOR in 0.01 M of Na_2SO_4 background solution, pH 4 at 25 °C.

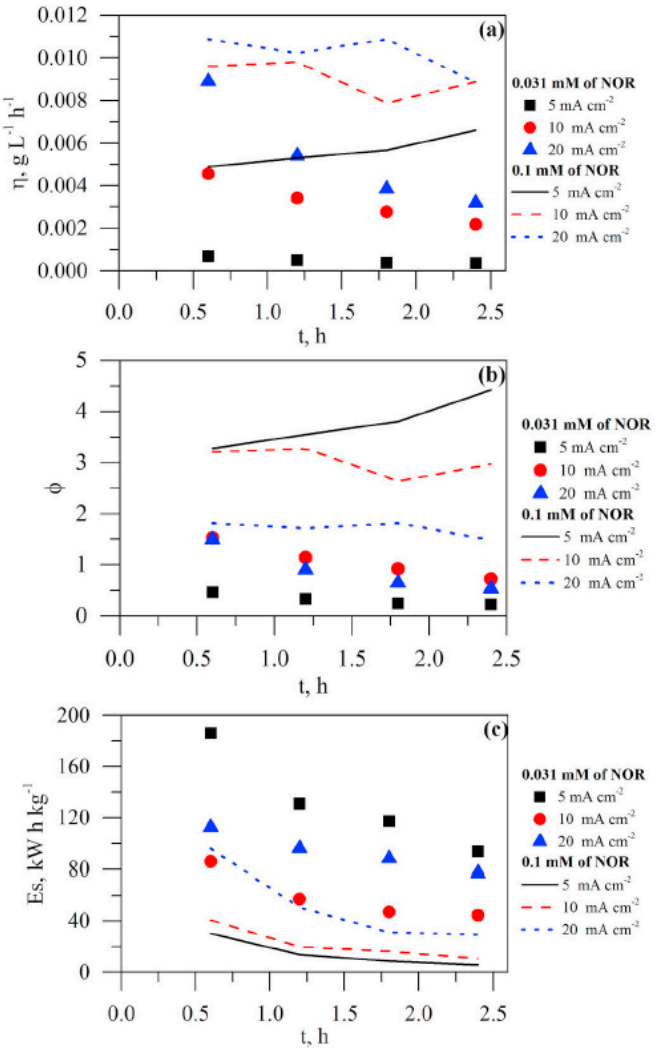

Fig. 7. Effect of the NOR concentration and i_{app} in the (a) space-time yield (η), (b) current efficiency (ϕ) and (c) specific energy consumption (E_s). EAOP initial conditions: 0.031 or 0.1 mM of NOR in 0.01 M of Na_2SO_4 background solution, pH 4 at 25 °C.

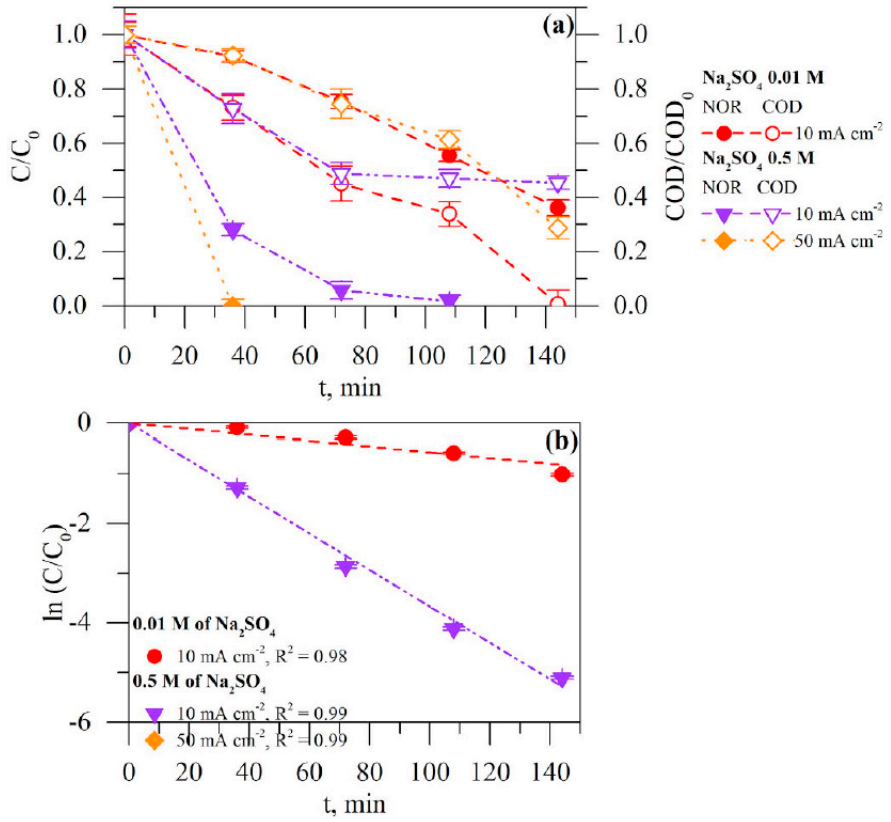

Fig. 8. Influence of the supporting electrolyte concentration and i_{app} in the (a) NOR abatement and (b) COD removal. EAOP initial conditions: 0.1 mM of NOR in 0.01 or 0.5 M of Na_2SO_4 background solution, pH 4 at 25 °C.

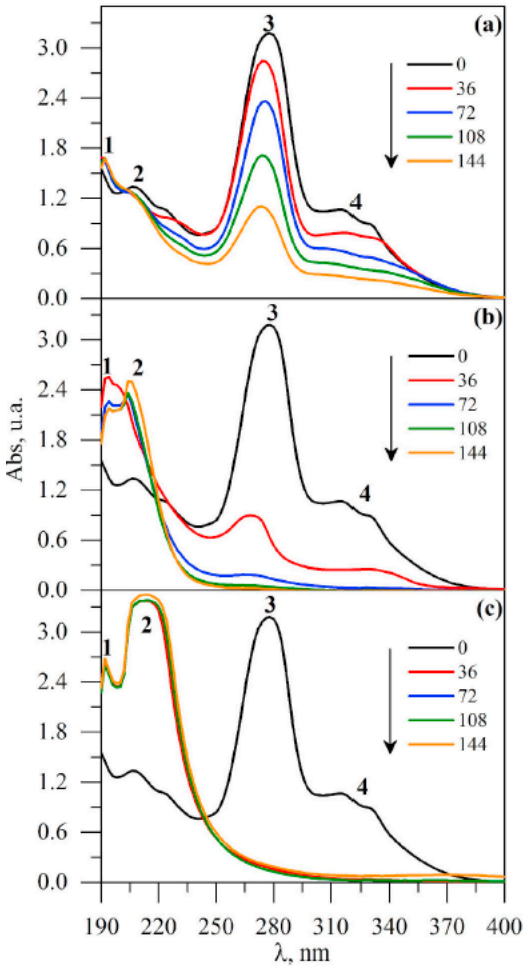

Fig. 9. Changes in UV/Vis spectra due to the influence of the supporting electrolyte concentration and the i_{app}. Electrolysis carried out at (a) 0.01 M of Na_2SO_4 and 10 mA cm^{-2}, (b) 0.5 M of Na_2SO_4 and 10 mA cm^{-2} and (c) 0.5 M of Na_2SO_4 and 50 mA cm^{-2}. EAOP initial conditions: 0.1 mM of NOR, pH 4 at 25 °C.

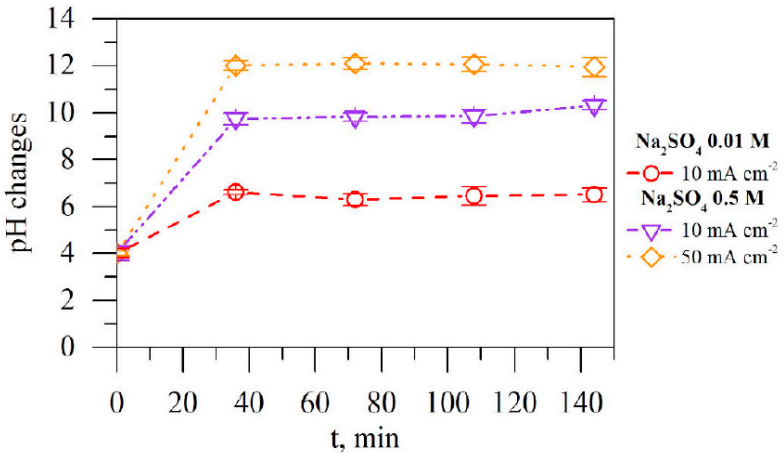

Fig. 10. pH changes as a function of the supporting electrolyte and the i_{app}. EAOP initial conditions: 0.1 mM of NOR in 0.01 or 0.5 M of Na_2SO_4 background solution, pH 4 at 25 °C.